Eur. Phys. J. B **69**, 237–244 (2009)
DOI: 10.1140/epjb/e2009-00138-y

THE EUROPEAN PHYSICAL JOURNAL B

Regular Article

Binding energy of hydrogenic impurity states in an inverse parabolic quantum well under static external fields

S. Baskoutas[1,2] and A.F. Terzis[3,4,a]

[1] Max Planck Institute for Solid State Research, Heisenbergstraße 1, 70569 Stuttgart, Germany
[2] Department of Materials Science, School of Natural Sciences, University of Patras, Rion, 26504, Greece
[3] Department of Physics, University of Cyprus, 1678 Nicosia, Cyprus
[4] Department of Physics, School of Natural Sciences, University of Patras, Rion, 26504, Greece

Received 23 January 2009
Published online 18 April 2009 –

Abstract. In the present theoretical study, we investigate the influence of external fields (electric and/or magnetic) on the binding energy of hydrogenic impurities in a GaAs/$Ga_{1-x}Al_xAs$ inverse parabolic quantum well, in which the parabolicity depends on the Al concentrations at the well center. Our calculations have been based on the potential morphing method in the effective mass approximation. The systematic theoretical investigation contains results with all possible combinations of the involved parameters, as quantum well width, Al concentrations at the well center, position of the impurity and magnitudes of the external fields.

PACS. 68.65.Fg Quantum wells – 61.72.-y Defects and impurities in crystals; microstructure – 83.60.Np Effects of electric and magnetic fields

1 Introduction

One of the main motivations behind the widespread interest in the physics of semiconductor hetero-structures lies in the ability of producing quantum confined systems where carriers are restricted to move in less than three dimensions. Structures produced by ultrathin-film growth are inherently two dimensional, as we grow one layer after the other. In these two dimensional structures, known as quantum well, only one direction (the growth direction) is quantized. Several investigations, experimental and theoretical have been devoted to this kind of hetero-structures [1–3]. Due to their small size these structures present physical properties that are quite different from those of the bulk semiconductor constituents [2–5].

Owing to advances in nanofabrication technology, it has become possible to manufacture high-quality semiconductor quantum wells with desired shape of the confinement potential. Apart from the well-known and well-studied quantum well hetero-structures (QWHs), which have square [3,6] and parabolic [3,7–10] potential shape, cases of QWHs with half parabolic [11], graded [12], V-shaped [13] and inverse parabolic quantum well (IPQW) potential shape [14–19] have been produced and studied.

Among the most important technological advances in the development of semiconductors as electronic materials, is the ability to introduce impurities directly into the lattice. The hydrogenic impurities play a crucial role in the design of nano-structured semiconductor materials, due to the fact that they affect strongly their optical and electronic properties, such that to suit the engineer's needs [3,9,18,20–28]. In addition, their influence can be controlled by the presence of external fields. Several articles have been published on the influence of external static (electric and magnetic) fields on hydrogenic impurities [10–13,17–19,29–35].

Especially, the IPQW give the possibility to realize high-performance optoelectronic devices. One reason for this has to do with the fact that is has a much larger amplitude reduction rate of the excitonic resonance than quantum wells of other shape. This originates from the quicker decrease in the overlap of the electron and heavy hole wave functions with the applied electric field. Actually this feature is much desirable for the quantum-confined field-effect light emitter and in the study of the confined Stark effect [15]. Although IPQW presents large interest, the existing literature on its fundamental physical properties is very limited [14–19].

In the present work, we study for the first time the influence of a magnetic field-perpendicular and/or parallel to the growth direction as well of a DC electric field along the growth direction on the binding energy of the hydrogenic impurities in a GaAs/$Ga_{1-x}Al_xAs$ IPQW, with different widths as well as different Al concentrations at the well center. Introduction of magnetic fields with various directions (parallel or perpendicular to the growth

[a] e-mail: terzis@physics.upatras.gr

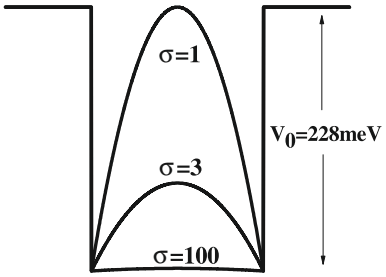

Fig. 1. Schematic shape of the inverse parabolic quantum well for various values of the σ-parameter (see Eq. (2), the well has width L).

direction) produces different kinds of confinement and therefore gives different behaviors of the hydrogenic impurity binding energy as a function of the impurity position. Our calculations will be based on the potential morphing method (PMM) [27,33,36,37], an accurate numerical method which has been developed in order to solve the time independent Schrödinger equation for any arbitrary interaction potential.

2 Theory

The Hamiltonian of the system in three-dimensions is given by the following expression in the effective mass approximation

$$H = \frac{1}{2m_e^*}\left[\vec{p}_e + \frac{e}{c}\vec{A}(\vec{r}_e)\right]^2 + V(z_e) - \frac{e^2}{\varepsilon\left|\vec{r}_e - \vec{r}_i\right|} + eE(z_e - z_i) \quad (1)$$

where E is magnitude of the external electric field which is applied along the z-axis, $\vec{A}(\vec{r}_e) = \left(\vec{B} \times \vec{r}_e\right)/2$ is the vector potential, $\vec{r}_e$ is the position vector of the electron, $\vec{r}_i$ is the position vector of the impurity and $\vec{B}$ the applied magnetic field. The origin of the x-y plane has been defined on the donor atom for convenience and without loss of generality. z_e is the position of the electron along the z-axis, z_i is the position of the impurity along the z-axis and $V(z_e)$ is the confinement potential profile for the electron in the z-direction. The confinement potential has the form [15,17]

$$V(z_e) = \begin{cases} \frac{V_0}{\sigma}\left(1 - \left(\frac{z_e}{L/2}\right)^2\right), & |z_e| \le L/2 \\ V_0 & |z_e| > L/2 \end{cases} \quad (2)$$

where $\sigma = x_{max}/x_c$ (x_{max} is the constant Al concentration at the barriers, x_c the Al concentration at the well center), V_0 is the band discontinuity for $x_{max} = 0.3$ [15,17], V_0/σ is the maximum value of the potential at the center of IPQW and L is the width of IPQW. The confinement potential is plotted in Figure 1, for the three values of σ used in our calculations. The case with the largest $\sigma(=100)$, is practically a square well.

In order to obtain the ground state of the Hamiltonian (1), we are using the PMM method with initial wavefunction the ground state of the usual three dimensional harmonic oscillator. Furthermore, the binding energy is defined as follows

$$E_b = E_0 - \overline{E} \quad (3)$$

where $\overline{E}$ is the energy which corresponds to Hamiltonian (Eq. (1)) and E_0 is the energy without Coulomb interaction (absence of third term in Hamiltonian of Eq. (1)).

The material parameters which have been used in our calculations are the following [17,38]: $m_e^* = 0.067m_0$ (where m_0 is the free electron mass), $\varepsilon = 12.5$ (considering that there is no dielectric constant mismatch) and $V_0 = 228$ meV [17]. As for the GaAs system the Bohr radius is such that it contains a significant number of atoms, it is apparent that the electromagnetic properties of the nanostructure are quite similar to the bulk material and the use of the static dielectric constant ($\varepsilon = 12.5$) is legitimate.

3 Results and discussion

First, in order to check the validity of our method and the effectiveness of our PMM codes in the case that an external magnetic field is present, we estimate the E_0 energy for a system characterized by an extremely large $\sigma(\to \infty)$, which (for vanishing external electric field) is identical to the prototype system studied in the book by Paul Harrison [3] and we find excellent agreement (Fig. 2.40 at p. 70 in Ref. [3]).

3.1 Zero electric field

3.1.1 Zero magnetic field

We start with the case with the largest $\sigma(=100)$, which is practically a square well. First we find that as the width of the well increases the binding energy of the donor impurity reaches its bulk value. Actually, for a value of $L = 20$ nm the binding energy is already very close to the bulk value (see solid curve in Fig. 2a). Moreover we find that the binding energy increases as the well width decreases; for example the binding energy for an impurity at the middle of the well with width $L = 20$ nm is 5.70 meV and for $L = 5$ nm is 20.54 meV. This is expected for the symmetric case of an impurity in the middle of the well, as with the decrease of the size of the well the 'effective' Bohr radius of the electron of the donor impurity becomes smaller, as the region of non-vanishing wave function of the electron decreases, and hence the Coulomb potential energy becomes larger. Obviously this behavior is more pronounced for sizes of the well smaller than the impurity Bohr radius in the bulk. As the donor Bohr radius for GaAs is 9.8 nm, the effects are stronger for L smaller than twice the Bohr radius.

In Figure 2, we plot the binding energy of the donors as a function of the position of the impurity in the well for a well with $L = 20$ nm. In Figure 2a we clearly see

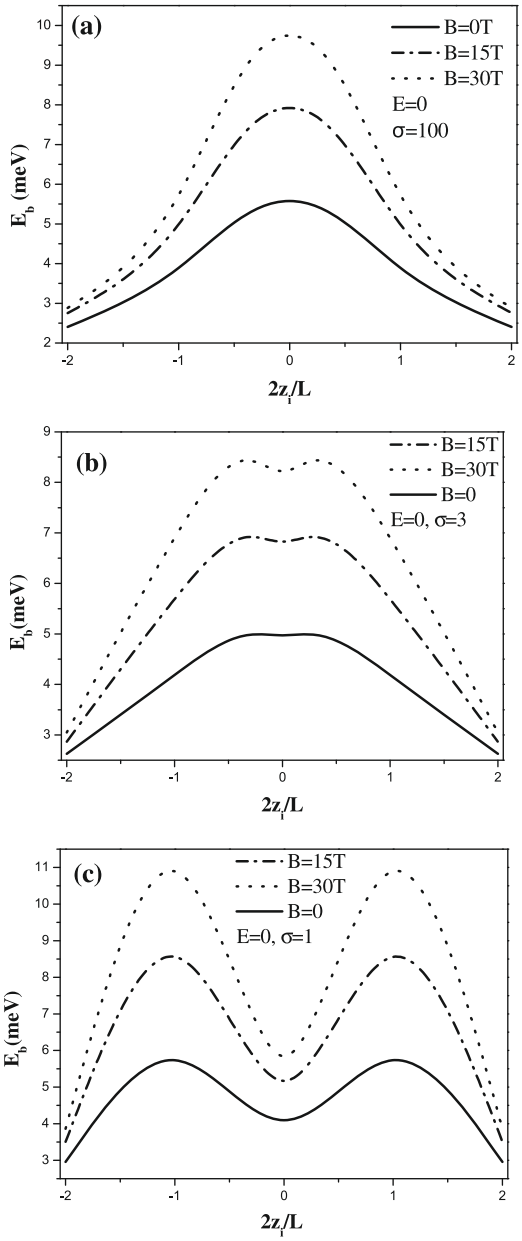

Fig. 2. Impurity binding energies as a function of the scaled position of the impurity in the IPQW structure for various magnetic fields. The magnetic field is parallel to the growth direction and there is no electric field. The quantum well width is 20 nm. The case studied corresponds to various shapes of the IPQW (a) $\sigma = 100$, (b) $\sigma = 3$ and (c) $\sigma = 1$.

that for the case of square well ($\sigma = 100$), the binding energy decreases as the position of the donor becomes more off-centered (i.e. as it approaches the barrier). This is explained once we understand that the 'effective' Bohr radius becomes larger for donors closer to the barrier. This means that once the donor is at the middle of the well the 'effective' Bohr radius is of the order of $L/2$, but once it is very close to the edge of the well the 'effective' Bohr radius is larger (it has a vanishing probability for entering remote regions in the barrier but on the contrary the electron can reach all the region in the well, with size of order of L).

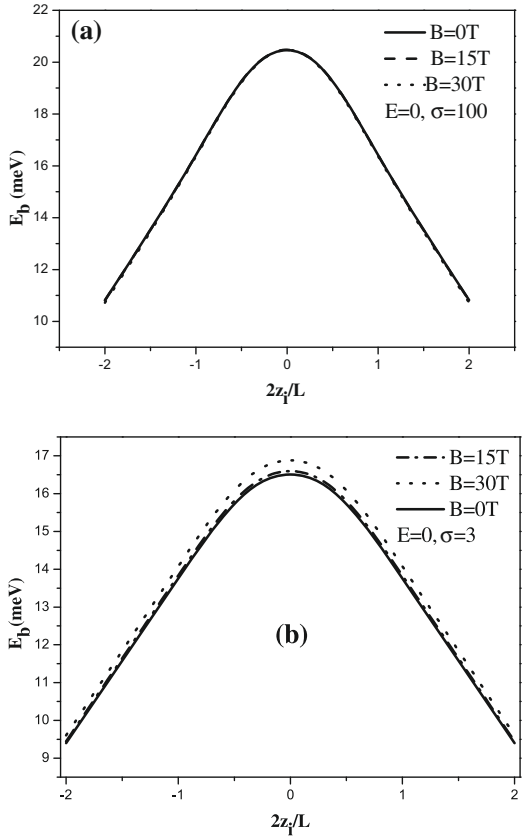

Fig. 3. Impurity binding energies as a function of the scaled position of the impurity in the IPQW structure for various magnetic fields. The magnetic field is parallel to the growth direction and there is no electric field. The quantum well width is 5 nm. The case studied corresponds to various shapes of the IPQW (a) $\sigma = 100$ and (b) $\sigma = 3$.

From Figures 2b and 2c we observe that once the shape of the well changes, the behavior of the binding energy as a function of the position changes. For $\sigma = 3$ (solid curves in Fig. 2b), where the deviation from the flat structure is not very significant, the behavior is similar to the one observed for flat well structure (solid curves in Fig. 2a). We only find that when the impurity is placed in the region around the center the binding energy is practically unchanged (region $[-L/4, L/4]$). But for the case with large deviation from the flat structure ($\sigma = 1$, see Fig. 2c), we find that the maximum of the binding energy is achieved for off-center positions of the donor. This is explained once we realize that the central region of the well, in this inverse parabolic well for small σ is a forbidden region for the electron (see Fig. 1, $\sigma = 1$). Actually the smaller the σ-parameter is the larger the region in the middle of the well that acts as a barrier. For low values of σ, it is practically as we have a symmetric two wells structure (see Fig. 1). With this in mind it becomes obvious why the maximum of the binding energy occurs at symmetric position close to the middle of these symmetric two well structures (i.e. it is as we have Fig. 2a repeated twice since we now have practically two wells).

In Figure 3, we investigate the case of $L = 5$ nm. First we confirm that the binding energy increases as the size

of the well decreases (compare Figs. 2 and 3). Then, in this case ($L = 5$ nm) for vanishing electric and magnetic field, we find that for all cases the behavior is as the one reported in Figure 2a. This means that no matter how large is the inverse parabolic barrier (i.e. how small is the σ-parameter), the binding energy always decreases, as the position of the donor gets closer to the AlAs barrier. Moreover, for $L = 5$ nm, we find that by decreasing the σ-parameter the binding energy becomes smaller (compare Fig. 3a with $\sigma = 100$ and Fig. 3b with $\sigma = 3$). This is explained by simply realizing that as the well becomes very narrow the ground state energy of the electron becomes very high with a value close to the barrier potential energy (for example for $\sigma = 100$ the ground state energy is $E_0 = 130.98$ meV and for $\sigma = 3$ the ground state energy is $E_0 = 173.24$ meV). This results in having an electron wavefunction that penetrates greatly into the barrier (even the barrier of the inverse parabolic region) and therefore the Coulomb interaction diminishes.

3.1.2 Magnetic field parallel to the growth direction

For an applied magnetic filed parallel to the growth direction (z-axis) the vector potential $\vec{A}$ can be written in the form $\vec{A}(\vec{r}_e) = -(\vec{r}_e \times B\hat{z})/2 = (-By_e/2, Bx_e/2, 0)$. The presence of the vector potential changes the kinetic energy of the electrons, but not the effective potential. This is still a symmetric potential, as it is expected for the present system. In Figures 2 and 3, we plot the binding energy of the system as a function of the position of the impurity. As the potential is symmetric with respect to the middle of the well, we expect and find all plots to be symmetric.

We find that as the magnetic field increases the binding energy increases. First we think that the increase of the binding energy with the presence of the field comparing to the case of no field, is expected, as a magnetic field parallel to the growth (z-axis) results in a restriction of the motion of the electron in the x-y plane. Having in mind that cyclotron frequency is proportional to B and cyclotron radius is inverse proportional to B, we can describe the observed behavior in two terms. One way of reasoning, is by realizing that for $\vec{B}$ parallel to $\hat{z}$, the 'effective' Bohr radius of the ground state reduces. The other way, is by observing that kinetic term is increased (see Eq. (1)), which is effectively equivalent to a decrease of the 'effective' Bohr radius. For the case of $L = 20$ nm, we observe that the binding energy increases much more for on-center donors than for off-center donors for rather flat wells (Figs. 2a and 2b) and that the binding energy increases much more for donors at positions close to $\pm L/2$ than for donors at other positions for non-flat wells (Fig. 2c). This is due to the fact that the confinement (presence of the barrier close to the impurity) is much more important than the effect of the field for very off-centered donors. This is in accordance to the picture we see for the case $L = 5$ nm (where the barrier effect is the major one).

But for the $L = 5$ nm case, the results suggest that the motion of the electron captured by the donor nucleus does not depend on the strength of the magnetic field. This is happening because in this case the restriction of the motion is mainly due to the confinement set by the barriers and not by the magnetic field (only minor changes are observed in the plots, with the correct trend, see Fig. 3b).

3.1.3 Magnetic field perpendicular to the growth direction

For an applied magnetic filed vertical to the growth direction (for example, parallel to the x-axis) the vector potential $\vec{A}$ can be written in the form $\vec{A} = (0, Bz_e/2, -By_e/2)$. We restrict to the case of $L = 20$ nm (Fig. 4), as the case of $L = 5$ nm does not shows any interesting effects (behavior similar to the case of parallel magnetic field, see Fig. 3).

In the study of this case we observe two interesting results. First, the increase in the binding energy with the increase of the applied magnetic field is always smaller in this case comparing to the case where the field is parallel to the growth direction. This is expected as the magnetic field produces a parabolic confinement along the directions perpendicular to the field direction. Hence in the case of $\vec{B}$ parallel to $\hat{z}$ the magnetic field produces a confinement along the x- and y-directions and leaves the third direction (z) being restricted exclusively by the well confinement. But in the case of $\vec{B}$ parallel to $\hat{x}$ the magnetic field produces a parabolic confinement along the y- and an additional confinement along z-directions and leaves the third direction (x) being practically unrestricted. Moreover, as σ decreases the binding energy decreases. This result is in agreement with the finding of the previous case study ($\vec{B}$ parallel to $\hat{z}$, see Figs. 2a and 2b). Additionally as is clearly seen from Figure 4a, an increase of the magnetic field increases the binding energy for flat wells. A decrease also of the σ-parameter ($\sigma = 3$) does not change the above mentioned behavior as is shown in Figure 4b. For very large magnetic fields ($B = 30$ T) the binding energy also increases but now in the plot appear two maxima with a value at $z_i = 0$ equal to the binding energy which corresponds to the other two magnetic fields, $B = 0$ and $B = 15$ T. This is expected due to the fact, as is also shown in the insets of Figure 4b, that it is possible to have a bound state at the point $z_e = 0$ where the confinement from the external applied magnetic field is equal to zero. Finally, in Figure 4c, the case of $\sigma = 1$ shows that increase of the magnetic field decreases the binding energy. For the ground states with energy below the barrier this behavior is due to the fact that an increase of the magnetic field creates electron wavefunctions which penetrate greatly into the barrier and therefore the binding energy decreases (case 1 in inset of Fig. 4c). For the ground states with energy above the barrier the observed behavior can be attributed to the fact that the electron "sees" a (effective) larger well (case 2 in inset of Fig. 4c). We point out, that our findings are in agreement with results reported by other researchers in reference [17].

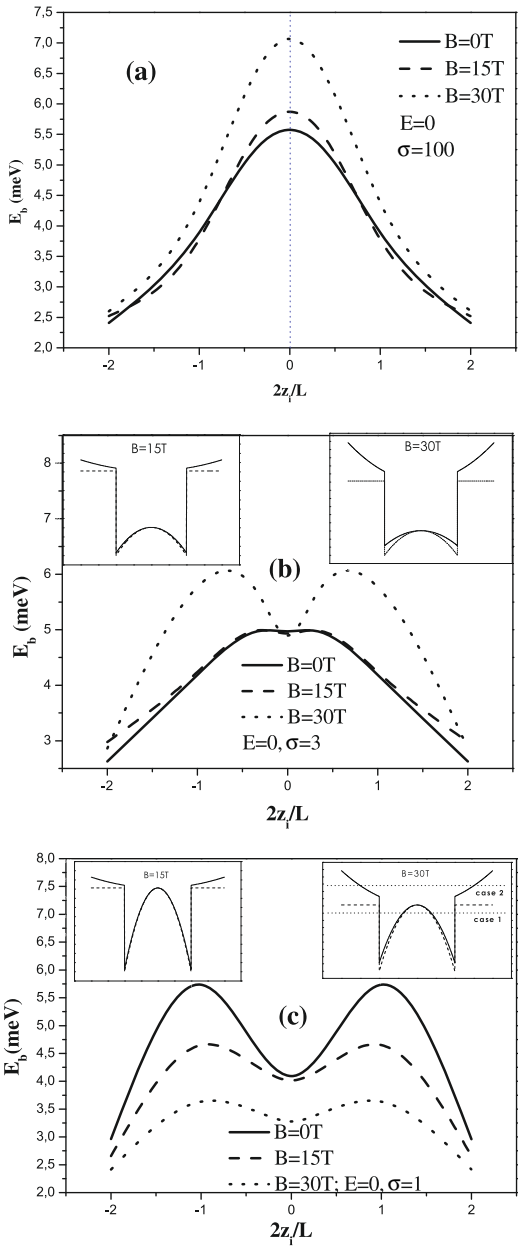

Fig. 4. Impurity binding energies as a function of the scaled position of the impurity in the IPQW structure. All parameters and cases studied are as in Figure 2, but the direction of the magnetic field is along the x-direction.

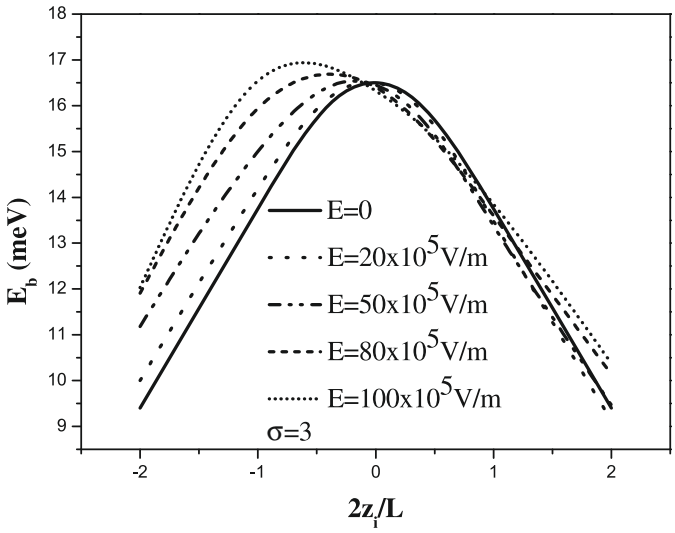

Fig. 5. Impurity binding energies as a function of the scaled position of the impurity in the IPQW structure for various electric fields. The magnetic field is zero. The quantum well width is 5 nm and $\sigma = 3$.

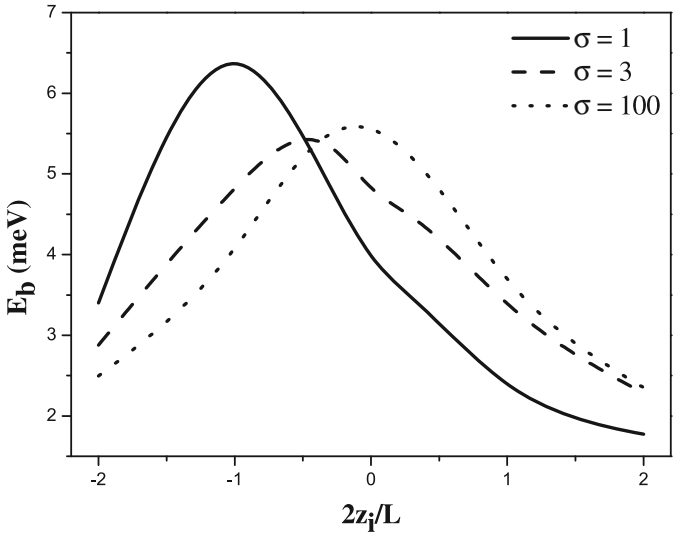

Fig. 6. Impurity binding energies as a function of the scaled position of the impurity in the IPQW structure shapes of the well. The magnetic field is zero and the electric field is 6×10^5 V/m. The quantum well width is 20 nm.

3.2 Finite electric field

First we study the case of zero magnetic field [18]. Once we have a non-zero electric field the quantum well structure becomes asymmetric. Presenting results for very narrow well, $L = 5$ nm, in Figure 5 and relatively wide well, $L = 20$ nm in Figure 6, we see that the effect of the asymmetry, depends strongly on the size of the well. For the case $\sigma = 3$, we clearly see from Figure 5 ($L = 5$ nm) that in order the electric field effects to be significant we need to apply a rather strong field. This is due to the fact that for such a narrow well the confinement is the most important factor on the binding energy. On the contrary, as it is seen in Figure 6 for the well with width $L = 20$ nm, for even a rather low field ($E = 6 \times 10^5$ V/m), the effect on the binding energy is significant. They are even present in the case of flat well (dotted curve in Fig. 6). This is explained by means of Figure 7c, where we see that the presence of an electric field changes the shape of the well so that it is like we have two wells, the one with lower energy than the other (one is deeper).

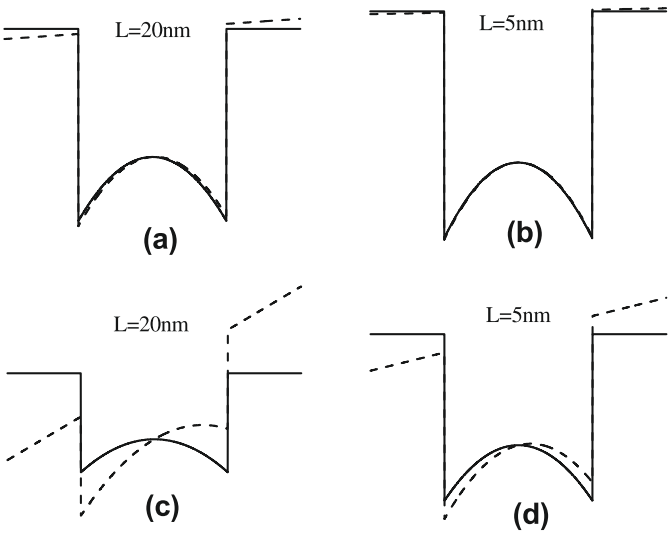

Fig. 7. Schematic shape of the inverse parabolic quantum well for $\sigma = 3$ and various electric fields. (a) $E = 6 \times 10^5$ V/m, $L = 20$ nm, (b) $E = 6 \times 10^5$ V/m, $L = 5$ nm, (c) $E = 10^7$ V/m, $L = 20$ nm and (d) $E = 10^7$ V/m, $L = 5$ nm.

3.2.1 Magnetic field parallel to the growth direction

In Figure 8 we plot the cases with magnetic filed parallel to the growth direction for a well width $L = 20$ nm. In the study of this case we report two significant findings. First, as we have explained before, the asymmetry, which appears in the form of the binding energy arises from the asymmetric form of the quantum well, even in the presence of a rather low field ($E = 6 \times 10^5$ V/m). This asymmetry of the well (which is more clear for the case $\sigma = 1$) causes a localization of the electron wavefunction on the left hand side of the well (which is deeper) and therefore this results in an increase of the binding energy in contrast with the right hand side where the binding energy decreases. Second, as the magnetic field increases the binding energy increases for the same reasons we have explained in Section 3.1.2.

3.2.2 Magnetic field perpendicular to the growth direction

For this case we have depicted in Figure 9 the behavior of the binding energy as a function of the impurity position for $\sigma = 100$, 3, 1. As is seen from Figure 9a ($\sigma = 100$) an increase of the magnetic filed causes an increase of the binding energy but this increase is smaller than the corresponding value for a magnetic field parallel to the growth direction which this is attributed to the larger confinement which is caused by the parallel magnetic field. Furthermore, as is seen from Figure 9b ($\sigma = 3$) for position of the impurity at the left hand side of the well, as the magnetic field increases the binging energy increases. But for positions of the impurity at the right hand side, as magnetic field increases the binding energy decreases. This is due to the asymmetry of the potential which increases the possibility to have states which penetrate more in the barrier material with the increase of the

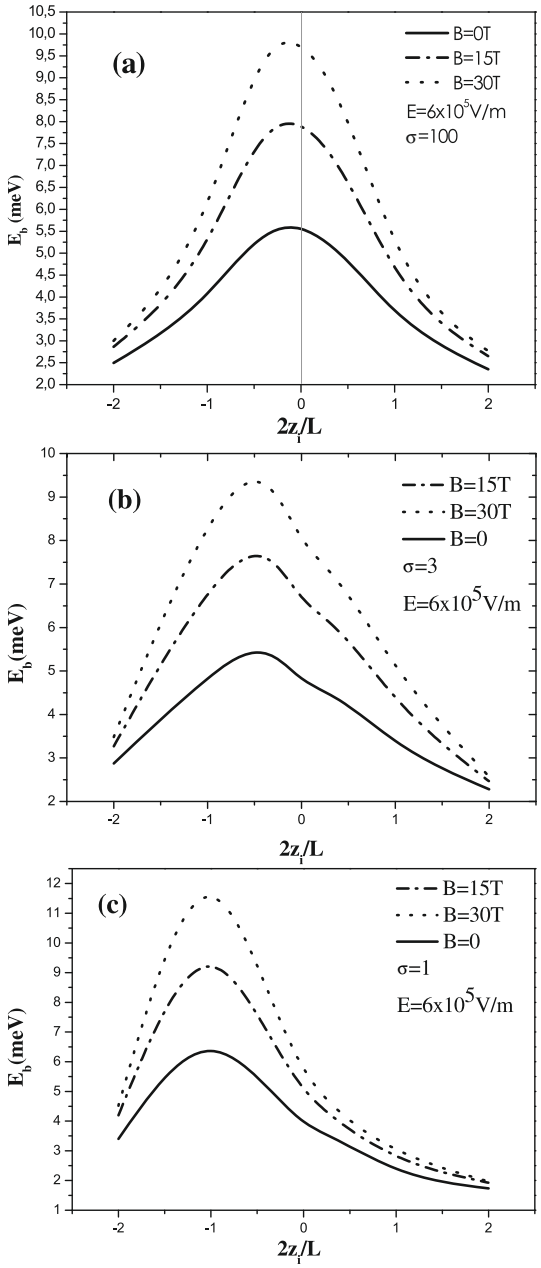

Fig. 8. Impurity binding energies as a function of the scaled position of the impurity in the IPQW structure for various magnetic fields. The magnetic field is parallel to the growth direction and the electric field is $E = 6 \times 10^5$ V/m. The quantum well width is 20 nm. The case studied correspond to various shapes of the IPQW (a) $\sigma = 100$, (b) $\sigma = 3$ and (c) $\sigma = 1$.

magnetic field for positions of the impurity on the right side of the well. Additionally, as we have explained before in Section 3.1.3, for positions of the impurity around zero the binding energies for the three values of the magnetic field are equal. Finally as is shown in Figure 9c ($\sigma = 1$), for positions of the impurity on the left side of the well, an increase of the magnetic field decreases the binding energy due to the fact that an increase of the magnetic field creates electron wavefunction, which penetrate greatly into

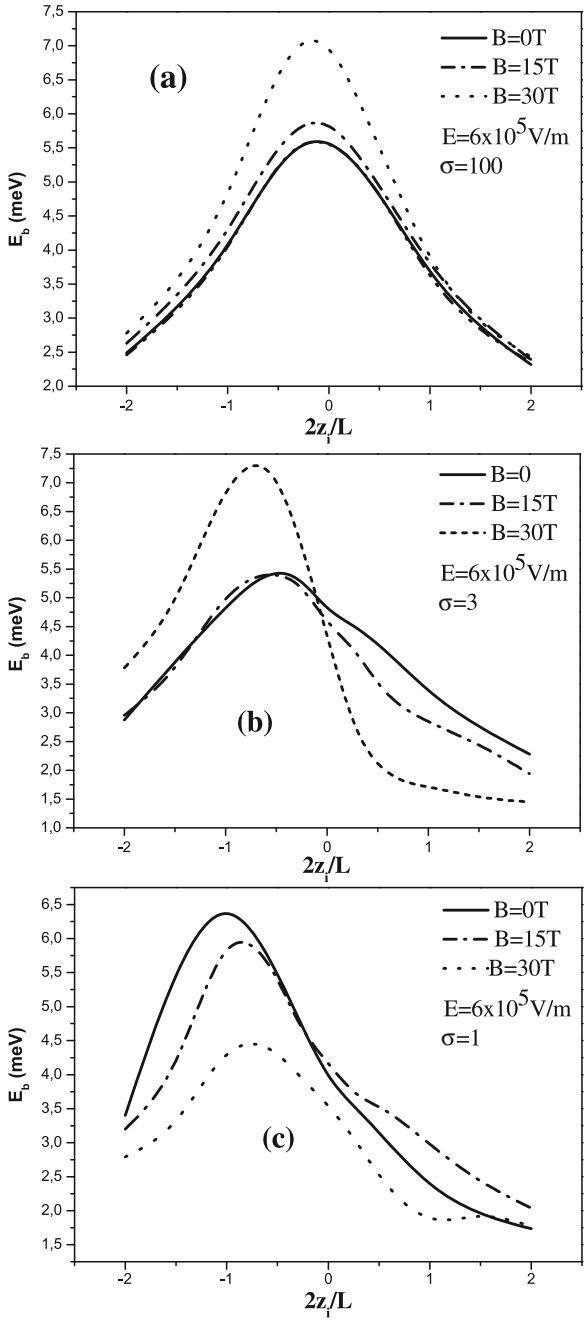

Fig. 9. Impurity binding energies as a function of the scaled position of the impurity in the IPQW structure for various magnetic fields. The magnetic field is perpendicular to the growth direction and the electric field is $E = 6 \times 10^5$ V/m. The quantum well width is 20 nm. The case studied corresponds to various shapes of the IPQW (a) $\sigma = 100$, (b) $\sigma = 3$ and (c) $\sigma = 1$.

the barrier. But for positions of the impurity on the right side the above mentioned behavior appears for magnetic fields greater than 25 T (not shown).

In the cases studied in Figures 8 and 9, the major difference is related to the trends of the binding energy with magnetic field magnitude (i.e. as the magnetic field increases the same occurs for the binding energy for magnetic field parallel to the growth direction, but for direction of the field perpendicular to the growth direction the opposite occurs). This behavior is understood in two terms. First, by means of the fact that the system of Figure 8 is more confined (confinement in three directions) comparing to the system of Figure 9 (confinement in two directions, i.e. y- and z-direction if the field is along x-axis). Second, the difference can be understood by means of Figure 10, where we show the shape of the effective potential that feels an electron in the IPQW structure when both fields are applied. The basic difference is found in states assigned as case2 in Figure 10, which describe cases with energies larger than the height of the 'natural' barrier ($V_0 = 228$ meV). In the system with magnetic field parallel to the growth direction, case2 does not correspond to bound states (Fig. 10a). On the contrary, in the system with magnetic field perpendicular to the growth direction, case2 describes bound states (confined by the parabolic potential along the z-direction, Fig. 10b). As is easily seen for this case the effective width of the well increases and therefore the binding energy decreases comparing with the case where magnetic field is equal to zero.

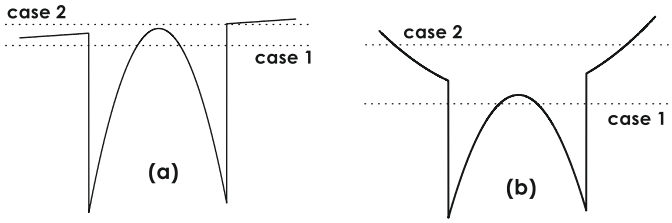

Fig. 10. Schematic shape of the inverse parabolic quantum well with width $L = 20$ nm for $\sigma = 1$ and electric field $E = 6 \times 10^5$ V/m. (a) magnetic field parallel to the growth direction (any field value gives the same shape in the z-direction) and (b) magnetic field perpendicular to the growth direction, $B = 30$ T.

4 Conclusions

Using the potential morphing method in the effective mass approximation, we have studied fundamental physical properties of a GaAs/$Ga_{1-x}Al_xAs$ inverse parabolic quantum well, by investigating the effects of external fields on the binding energy of hydrogenic impurities present in the well. The fields applied are magnetic fields parallel or perpendicular to the growth direction and DC electric field along the growth direction. We study wells of various sizes and shapes (the shape of the inverse parabolic quantum well is controlled by the Al concentrations at the well center). Our results indicate, concerning the behavior of the binding energy as a function of the impurity position, that the existence of the electric field causes an asymmetry on the binding energy, which is stronger for intermediate confinements. Furthermore we have found that the binding energy depends strongly on the different Al concentrations at the well center, the length of the quantum well as well as on the magnetic filed. As it is expected, it shows different behavior for different

direction (parallel/perpendicular to the growth direction) of the magnetic field.

We believe that our results can be helpful not only in the elucidation of the fundamental physics of the system but also in the design of inverse parabolic quantum wells with new and interesting optoelectronic properties.

References

1. A.D. Yoffe, Adv. Phys. **42**, (1993) 173
2. G. Bastard, *Wave Mechanics Applied to Semiconductor Heterostructures* (Les Éditions de Physique, Les Ulis, 1988)
3. P. Harrison, *Quantum Wells, Wires and Dots* (Wiley, NY, 2006)
4. L.L. Chang, L. Esaki, R. Tsu, Appl. Phys. Lett. **24**, 593 (1974)
5. R. Dingle, A.C. Gossard, W. Wiegmann, Phys. Rev. Lett. **33**, 827 (1974)
6. C. Mailhiot, Yia-Chung Chang, T.C. McGill, Phys. Rev. B **26**, 4449 (1982)
7. R.C. Miller, A.C. Gossard, O.A. Kleinman, O. Munteanu, Phys. Rev. B **29**, 3740 (1984)
8. Q. Guo, Y.P. Feng, H.C. Poon, C.K. Ong, Eur. Phys. J. B **9**, 29 (1999)
9. F.Q. Zhao, X.X. Liang, S.L. Ban, Eur. Phys. J. B **33**, 3 (2003)
10. Z.P. Wang, X.X. Liang, X. Wang, Eur. Phys. J. B **59**, 41 (2007)
11. Y.-B. Yu, S.-N. Zhu, K.-X. Guo, Phys. Lett. A **335**, 175 (2005)
12. E. Kasapoglu, H. Sari, I. Sökmen, Surf. Rev. Lett. **13**, 397 (2006)
13. E. Kasapoglu, I. Sökmen, Physica E **27**, 198 (2005)
14. K.K. Law, R.H. Yan, A.C. Gossard, J.L. Merz, J. Appl. Phys. **67**, 6461 (1990)
15. W.Q. Chen, S.M. Wang, T.G. Andersson, J.T. Thordson, Phys. Rev. B **48**, 14264 (1993); W.Q. Chen, S.M. Wang, T.G. Andersson, J.T. Thordson, J. Appl. Phys. **74**, 6247 (1993)
16. S. Vlaev, V.R. Velasco, F. Garcia-Moliner, Phys. Rev. B **51**, 7321 (1995)
17. E. Kasapoglu, H. Sari, I. Sökmen, Physica B **390**, 216 (2007)
18. S. Baskoutas, A.F. Terzis, Physica E **40**, 1367 (2008)
19. S. Elagoz, P. Baser, U. Yahsi, Physica B **403**, 3879 (2008)
20. N.W. Aschroft, N.D. Mermin, *Solid State Physics* (Saunders College Publishing, Philadelpia, 1976)
21. S.M. Sze, *Semiconductor Devices: Physics and Technology* (Wiley, NY, 1985)
22. G, Bastard, Phys. Rev. B **24**, 4714 (1981)
23. S.N. Chaudhuri, K.K. Bajaj, Phys. Rev. B **29**, 1803 (1984)
24. J.W. Brown, H.N. Spector, J. Appl. Phys. **59**, 1179 (1986)
25. R.L. Greene, K.K. Bajaj, Phys. Rev. B **37**, 4604 (1988)
26. M. Combescot, R. Combescot, B. Roulet, Eur. Phys. J. B **22**, 89 (2001)
27. S. Baskoutas, A.F Terzis, E. Voutsinas, J. Comp. Theor. Nanoscience **1**, 315 (2004)
28. D.N. Quang, L. Tuan, N.T. Tien, Phys. Rev. B **77**, 125326 (2008)
29. S.V. Branis, G. Li, K.K. Bajaj, Phys. Rev. B **47**, 1316 (1993)
30. W.Q. Chen, S.M. Wang, T.G. Andersson, J. Thordson, Phys. Rev. B **48**, 14264 (1993)
31. P. Villamil, N. Porras-Montenegro, J. Phys.: Condens. Matter **10**, 10599 (1998)
32. Z.X. Liu, Z.J. Lai, Y.C. Huang, Y. Liu, G.J. Cheng, Eur. Phys. J. B **12**, 347 (1999)
33. A.F. Terzis and S. Baskoutas, *Trends in Quantum Dot Research*, edited by P.A. Ling (Nova Science Publishers, New York, 2005), pp. 93–124
34. B. Chen, K.X. Guo, R.Z. Wang, Y.B. Zheng, B. Li, Eur. Phys. J. B **66**, 227 (2008)
35. K. Efstathiou, O.V. Lukina, D.A. Sadovskii, Phys. Rev. Lett. **101**, 253003 (2008)
36. S. Baskoutas, A.F. Terzis, J. Appl. Phys. **98**, 044309-1 (2005); S. Baskoutas, A.F. Terzis, J. Appl. Phys. **99**, 013708 (2006)
37. S. Baskoutas, E. Paspalakis, A.F Terzis, Phys. Rev. B **74**, 153306 (2006)
38. S. Adachi, J. Appl. Phys. **58**, R1 (1985)